Theoretical calculation of the pure electronic spectrum of MnF_6^{4-} *in vacuo* and in $RbMnF_3$

M. Flórez, L. Seijo,* and L. Pueyo
Departamento de Química Física, Facultad de Química, Universidad de Oviedo, E-33007 Oviedo, Spain
(Received 26 December 1984; revised manuscript received 23 January 1986)

The pure electronic d-d spectrum of the MnF_6^{4-} complex ion has been computed at different values of the Mn^{2+}-F^- distance R along the a_{1g} vibration mode, following an open-shell self-consistent-field—molecular-orbital (SCF-MO) methodology. Both cluster—*in-vacuo* and cluster—in-the-lattice ($RbMnF_3$) calculations have been performed in terms of rigid-lattice and partially-relaxed-lattice models. Theoretical spectral parameters have been obtained from the SCF results, and the evolution of the $3d$ splitting and the d-d repulsion with R has been examined. The lattice effects on the computed spectrum turned out to be very small in the present calculation. The overall description of the pure electronic single- and double-excitation transitions is rather good: sixteen transition energies are calculated with an rms deviation smaller than 1.9 kilokaysers (kK). This energy calculation partially supports the assignment of the peaks at (42—44) kK to double excitations. The energy splitting of the $^4A_{1g}$, $^4E_g^a$ states and its relationship with the electronic delocalization of the $3d$ MO's have been analyzed. The present calculation predicts, for MnF_6^{4-}, a variation of the $10Dq$ with R as $R^{-3.6}$ ($1.7 \leq R \leq 2.3$ Å), in agreement with the thermal expansion of the $RbMnF_3$ lattice, the red shifts shown by the lower quartets upon cooling, and the results of other theoretical calculations. Conversely, the Racah parameters B and C show a very slight and opposite variation with R.

I. INTRODUCTION

The optical spectrum of the MnF_6^{4-} complex ion has been extensively analyzed in MnF_2 (Refs. 1—16), manganese trifluorides, such as $KMnF_3$ (Refs. 7, 9, and 17—23), $RbMnF_3$ (Refs. 7, 9, 12, 14, 19, 20, and 24—26), $NaMnF_3$ (Ref. 27), $CsMnF_3$ (Refs. 7 and 28), and NH_4MnF_3 (Ref. 29), manganese tetrafluorides, like $BaMnF_4$ (Ref. 30), and in a variety of doped crystals, such as Mn^{2+}:$KMgF_3$ (Refs. 21 and 31—33), Mn^{2+}:$KZnF_3$ (Refs. 17—19 and 34), Mn^{2+}:$KCoF_3$ (Ref. 23), Mn^{2+}:ZnF_2 (Ref. 35), Mn^{2+}:MgF_2 (Ref. 36), Mn^{2+}:$RbMgF_3$ (Refs. 37 and 38), Mn^{2+}:NaF (Refs. 12 and 39), and Mn^{2+}:LiF (Ref. 39). The spectrum of the $RbMnF_3$ is possibly the more complete, because many single-excitation transitions,[25] and several double excitations above 38 kilokaysers (kK) (Ref. 14) have been observed at different temperatures.

These spectra can be rationalized in terms of the electronic energy levels of the MnF_6^{4-} cluster predicted by crystal-field theory. However, a more complete understanding can be obtained from a detailed calculation of the electronic structure of the cluster. From such calculation one can analyze (a) the interpretative capability of the Tanabe-Sugano matrices in terms of *nonempirical* spectral parameters, (b) the metal-ligand covalency, required, for instance, in the spectral assignment of the $^4E_g^a$,$^4A_{1g}$ multiplets, degenerate in crystal-field theory, (c) the spectral significance of the crystal lattice potential, and (d) the variations of the electronic transitions and the spectral parameters with the manganese-fluoride separation R.

These and other questions have been investigated in this work, from a Hartree-Fock-Roothaan (HFR) calculation of the electronic structure of MnF_6^{4-}, at several values of R, with different degrees of refinement. Although several calculations of this type have been reported for the MnF_6^{4-} unit, an overall study of the electronic spectrum and the questions listed above has not yet been given. Freeman and Ellis[40] and Soules and Richardson[41] reported self-consistent field (SCF) calculations on MnF_6^{4-} and discussed the neutron magnetic form factors. Matsuoka[42] studied the effects of different methodological improvements on the covalency parameters and $10Dq$. Lohr[43] discussed the relative position of the $^4E_g^a$,$^4A_{1g}$ states and showed that the $^4E_g^a$ cannot be below the $^4A_{1g}$ if reasonable covalency parameters were used. Larsson and Connolly[44,45] obtained good values for $10Dq$ and transferred hyperfine (thf) interaction parameters from multiple scattering $X\alpha$ calculations on MnF_6^{4-}. Adachi *et al.*[46] also found good descriptions for $10Dq$ and thf interaction parameters, and reported that the lattice potential of perovskite compounds improves the level structure of the cluster. Emery, Leble, and Fayet[47] and Emery and Fayet[48] also reported SCF calculations on MnF_6^{4-} *in vacuo* and within a lattice potential, but did not discuss the optical spectrum.

Our calculation has been carried out following the open-shell self-consistent-field—molecular-orbital (SCF-MO) methodology of Richardson *et al.*[49] This method has given very good results in a variety of spectral calculations on analogous systems.[50—55] Cluster—*in-vacuo* calculations, performed at eight values of the metal-ligand distance R, have been complemented with cluster—in-the-lattice calculations, in terms of rigid-lattice[56] and partially-relaxed-lattice models.[57,58] The vertical d-d spectrum at $R = 4.0$ a.u. (2.12 Å) has been computed with progressive levels of accuracy, including configuration interaction (CI) limited to the $t_{2g}^x e_g^y$ ($x+y=5$) configurations, and an empirical correction to the correlation ener-

gy error. From the vertical calculation we have computed theoretical spectral parameters by fitting the d^5 crystal-field matrices to the theoretically computed electronic transitions.[59,60] Furthermore, we have analyzed the R dependence of all the sextet-quartet electronic transitions of the d^5 configuration, and the spectral parameters from $R = 1.6$–2.3 Å. The relative position of the $^4A_{1g}$ and $^4E_g^a$ states has been studied within several covalency models and as a function of R.

The more important conclusions from this work are the following.

(a) The effects of the external lattice potential on the cluster—*in-vacuo* calculation were almost negligible, in contrast with the earlier results of Adachi *et al.*[46] and the recent study on the shared-cluster system CrF_3.[57] This result seems to be compatible with the fact that the pure electronic spectrum of MnF_6^{4-} recorded in many concentrated materials is very slightly dependent on the nature of the material.

(b) We obtained a rather good value for $10Dq$ at the equilibrium nuclear configuration of $RbMnF_3$ and described the optical spectrum of this system with a reasonable quality: We compute eight single-excitation and eight double-excitation transitions with a root-mean-square deviation smaller than 2 kK. Although we have not computed transition intensities in this paper, the theoretical transition energies and their variation with R partially support the assignment of the peaks above 38 kK to double excitation transitions.

(c) We obtained the theoretical R dependence of $10Dq$, compatible with the inverse power law $R^{-3.60}$, and, in good agreement with the observed values of the thermal expansion of the crystal, the red shifts of the low-energy single excitations upon cooling, and the theoretical results of Adachi *et al.*[46] Given the very small effects of the lattice potential, this R dependence could perhaps be useful for other manganese fluorides as well.

(d) We obtained the theoretical R dependence of the Racah electron-repulsion parameters B and C: They show a very slight and opposite variation with R in the range of values studied here.

(e) We obtained the relative position of the $^4E_g^a$, $^4A_{1g}$ states: Whereas the molecular-orbital description shows a splitting energy $\Delta E = E(^4E_g^a) - E(^4A_{1g})$ largely dependent on R and positive at the equilibrium configuration, the semiempirical, two-parameter covalency schemes earlier discussed in the literature predict a different variation of ΔE with R, and $\Delta E < 0$ at $R \simeq R_e$.

Finally, we notice that several questions related to the understanding of the optical spectrum of MnF_6^{4-}, such as the fine structure of the observed peaks and the intensity mechanisms, have not been discussed in this paper. Also, results of our theoretical calculation related to other electronic transitions, the $3d \rightarrow 4s$ and $3d \rightarrow 4p$ excitations, are not considered here and will be reported soon.

II. METHODOLOGY

SCF calculations have been performed for the electronic ground state, $t_{2g}^3 e_g^{2\,6}A_{1g}$, and the $t_{2g}^3 e_g^{2\,4}A_{1g}, t_{2g}^3 e_g^{2\,4}T_{1g}$ excited states at eight values of the metal-ligand internuclear distance R along the a_{1g} vibration mode. The atomic STO basis set for the Mn^{2+} ion has been taken from Richardson *et al.*[61,62] and the F^- Slater-type orbital (STO) basis from Ref. 53. Two different core-valence partitions have been considered within the frozen-core approximation.[49] In the SPDD partition the valence shell is composed of the $3s_M$, $3p_M$, $3d_M$, and $3d_I$ metal orbitals [$3d_I$ is the inner STO of the regular 2-ζ $3d$ function of Ref. 61] as well as the $2s_L$ and $2p_L$ ligand functions. In the partition called SPDDSP we extend the SPDD valence shell with the $4s$ and $4p$ metal orbitals, giving rise to the corresponding increase in the size of the a_{1g} and t_{1u} matrices. Adequate modifications in the original computer programs developed by Richardson and his co-workers have been introduced by one of us[63] in order to deal with the augmented matrices.

The spectral calculations have been performed, within the frozen-orbital approximation, by using the SCF solutions of the three electronic states considered here. Very slight differences are found among these three calculations. Thus, we will report results corresponding to the SCF solutions of the ground state.

To compute the electronic energies of the multiplets involved in this spectral calculation, multielectron open-shell MO wave functions defined over the t_{2g} (ξ,η,ζ) and e_g (θ,ϵ) MO's are required. We have obtained these functions following Griffith's choice of phase (Ref. 64, p. 396). They are collected in Table I. Since we limit the calculation to the sextet-quartet transitions, the doublet wave functions are omitted.

To complete the calculation we have to choose a set of ten independent e_g-t_{2g} electronic repulsion integrals.[64] In this work we have used the set introduced by Richardson *et al.*[49] A slightly different set was introduced by Griffith[64] and adopted by Sharma *et al.*[65,66] For an easy comparison we present in Table II the definitions of these sets and their mutual relationships.[49,64] When the t_{2g} and e_g functions are pure $3d$ atomic orbitals (AO's) these repulsion parameters reduce to linear combinations of the well-known Racah parameters A, B, and C. Such expressions are also shown in Table II. Notice that some of these relations appear in Table I of Ref. 49. Also, complete information on these parameters is given in Table A26 of Ref. 64. Spectral calculations have been done at several levels of approximation, as follows.

A. First-order calculation

At this level of approximation the electronic transition energies are computed as differences in total energies obtained from the diagonal matrix elements of the electron-interaction matrix. The appropriate energy expressions in terms of the parameters used in this work have been given by Richardson *et al.*[49] Using the MO wave functions of Table I we find energy expressions coincident with those in Ref. 49, as well as with those reported by Sharma *et al.*[65] These diagonal open-shell energies are collected in Table III. The Tanabe-Sugano expressions in terms of A, B, and C, collected in Table A30 of Griffith's book,[64] are obtained from those in Table III by taking the limit expressions given in Table II.

TABLE I. Open-shell MO wave functions corresponding to the sextet and quartets of the $t_{2g}^{x}e_g^{y}$ $(x+y=5)$ configurations. Note, only the components of maximum M_s are listed. For orbitally degenerate states, only one subspecies is shown.

$^6A_{1g}$	$\lvert t_{2g}^3(^4A_{2g})e_g^2(^3A_{2g})\frac{5}{2},a_1\rangle = -\lvert \xi\eta\zeta\theta\epsilon\rvert$ [a]
$^4A_{2g}$	$\lvert t_{2g}^3(^4A_{2g})e_g^2(^1A_{1g})\frac{3}{2},a_2\rangle = -(\lvert \xi\eta\zeta\theta\bar{\theta}\rvert + \lvert \xi\eta\zeta\epsilon\bar{\epsilon}\rvert)/\sqrt{2}$
$^4A_{1g}$	$\lvert t_{2g}^3(^4A_{2g})e_g^2(^3A_{2g})\frac{3}{2},a_1\rangle = (\frac{3}{10})^{1/2}[-\lvert \xi\eta\zeta\bar{\theta}\epsilon\rvert - \lvert \xi\eta\zeta\theta\bar{\epsilon}\rvert + 2(\lvert \bar{\xi}\eta\zeta\theta\epsilon\rvert + \lvert \xi\bar{\eta}\zeta\theta\epsilon\rvert + \lvert \xi\eta\bar{\zeta}\theta\epsilon\rvert)/3]$
^4E_g	$\lvert t_{2g}^3(^2E_g)e_g^2(^3A_{2g})\frac{3}{2},\theta\rangle = (2\lvert \xi\eta\bar{\zeta}\theta\epsilon\rvert - \lvert \xi\bar{\eta}\zeta\theta\epsilon\rvert - \lvert \bar{\xi}\eta\zeta\theta\epsilon\rvert)/\sqrt{6}$ $\lvert t_{2g}^3(^4A_{2g})e_g^2(^1E_g)\frac{3}{2},\theta\rangle = (\lvert \xi\eta\zeta\bar{\theta}\epsilon\rvert - \lvert \xi\eta\zeta\theta\bar{\epsilon}\rvert)/\sqrt{2}$
$^4T_{1g}$	$\lvert t_{2g}^4(^3T_{1g})e_g\frac{3}{2},z\rangle = \lvert \xi\eta\zeta\bar{\xi}\theta\rvert$ $\lvert t_{2g}^3(^2T_{2g})e_g^2(^3A_{2g})\frac{3}{2},z\rangle = (\lvert \xi\bar{\xi}\zeta\theta\epsilon\rvert + \lvert \eta\bar{\eta}\zeta\theta\epsilon\rvert)/\sqrt{2}$ $\lvert t_{2g}^2(^3T_{1g})e_g^3(^2E_g)\frac{3}{2},z\rangle = \lvert \eta\xi\theta\epsilon\bar{\epsilon}\rvert$
$^4T_{2g}$	$\lvert t_{2g}^4(^3T_{1g})e_g\frac{3}{2},\zeta\rangle = \lvert \xi\eta\zeta\bar{\xi}\epsilon\rvert$ $\lvert t_{2g}^3(^2T_{1g})e_g^2(^3A_{2g})\frac{3}{2},\zeta\rangle = (\lvert \xi\bar{\xi}\zeta\theta\epsilon\rvert - \lvert \eta\bar{\eta}\zeta\theta\epsilon\rvert)/\sqrt{2}$ $\lvert t_{2g}^2(^3T_{1g})e_g^3(^2E_g)\frac{3}{2},\zeta\rangle = \lvert \eta\xi\theta\bar{\theta}\epsilon\rvert$

[a]The notation $\xi\equiv\xi\alpha$, $\bar{\xi}\equiv\xi\beta$ is used.

B. Configuration interaction (CI) limited to the $t_{2g}^{x}e_g^{y}$ $(x+y=5)$ configurations

As in calculations performed in analogous systems, we see that the first-order calculation is significantly improved when configuration interaction within the open-shell configurations derived from the d^n case is considered. The required electrostatic matrices have been given by Sharma *et al.*,[65,66] in terms of the V_i parameters (Table II). We have computed the matrix elements of the quartets with the wave functions of Table I. They are listed in Table III.

C. Correlation energy correction (CEC)

This spectral correction to the nonempirical calculation of the electronic transition energies was introduced by Pueyo and Richardson[67] and turned out to be a significant improvement in spectral calculations on NiF_6^{4-} and CrF_6^{3-},[67] CrF_6^{4-},[54,63] and CrF_6^{2-}.[55] Briefly, the CEC eliminates from the cluster calculation the errors associated with the calculation of the free-ion SL term energies, after transformation from the SL space to the cluster $S\Gamma$ space: First, the matrix elements of the diagonal, free-ion CEC matrix are defined as the differences $E_{SL}(\text{calculated})-E_{SL}(\text{observed})$, referred to the ground term energy.[67] Then, this matrix is transformed into the cluster CEC matrix by means of a similarity transformation involving the matrix of the vector coupling coefficients $\langle iSL \mid t_{2g}^{x}e_g^{y}-jS\Gamma\rangle$ ($\mid iSL\rangle$ are the free-ion term wave functions and $\mid t_{2g}^{x}e_g^{y}-jS\Gamma\rangle$ are the strong-field, cluster wave functions). The cluster CEC matrix is then added up to the electrostatic interaction matrix $\underline{H}$ (the

TABLE II. Independent e_g-t_{2g} electronic repulsion integrals.

Integral[a]	Griffith (Ref. 64)	Sharma (Ref. 65)	Richardson (Ref. 49)[b]
$(\xi\xi\mid\xi\xi)$	$a\rightarrow A+4B+3C$	V_1	$\bar{J}(tt)=[(\xi\xi\mid\xi\xi)+(\xi\xi\mid\eta\eta)+(\xi\xi\mid\zeta\zeta)]/3$ $=(a+2b)/3\rightarrow A+5C/3$
$(\eta\eta\mid\xi\xi)$	$b\rightarrow A-2B+C$	V_2	$\bar{K}(tt)=[(\xi\xi\mid\xi\xi)+(\xi\eta\mid\xi\eta)+(\xi\zeta\mid\xi\zeta)]/3$ $=(a+2j)/3\rightarrow(A+10B+5C)/3$
$(\theta\epsilon\mid\xi\xi)$	$c\rightarrow 2B\sqrt{3}$	V_3	$K(tt)=j\rightarrow 3B+C$
$(\epsilon\epsilon\mid\xi\xi)$	$d\rightarrow A-2B+C$	V_4	$\bar{J}(et)=[(\xi\xi\mid\epsilon\epsilon)+(\xi\xi\mid\theta\theta)]/2$ $=d+c/\sqrt{3}\rightarrow A+C$
$(\theta\theta\mid\theta\theta)$	$e\rightarrow A+4B+3C$	V_5	$\bar{K}(et)=[(\xi\epsilon\mid\xi\epsilon)+(\xi\theta\mid\xi\theta)]/2$ $=g+h/\sqrt{3}\rightarrow 2B+C$
$(\theta\epsilon\mid\theta\epsilon)$	$f\rightarrow 4B+C$	V_6	$J(et)=d-c/\sqrt{3}\rightarrow A-4B+C$
$(\theta\eta\mid\theta\eta)$	$g\rightarrow B+C$	V_7	$K(et)=g+h\sqrt{3}\rightarrow 4B+C$
$(\theta\eta\mid\epsilon\eta)$	$h\rightarrow B\sqrt{3}$	V_8	$\bar{J}(ee)=[(\theta\theta\mid\theta\theta)+(\theta\theta\mid\epsilon\epsilon)]/2$ $=e-f\rightarrow A+2C$
$(\theta\xi\mid\eta\zeta)$	$i\rightarrow B\sqrt{3}$	V_9	$\bar{K}(ee)=[(\theta\theta\mid\theta\theta)+(\theta\epsilon\mid\theta\epsilon)]/2$ $=(e+f)/2\rightarrow(A+8B+4C)/2$[c]
$(\xi\eta\mid\xi\eta)$	$j\rightarrow 3B+C$	V_{10}	$i=(\theta\xi\mid\eta\zeta)=i\rightarrow B\sqrt{3}$

[a]$(ab\mid cd)=[a(1)b(1)\mid(1/r_{12})\mid c(2)d(2)]$.

[b]Used in this work.

[c]Note the misprint in the second equality shown in Table II of Ref. 49.

TABLE III. Diagonal and off-diagonal matrix elements of the sextet and quartet states of the $t_{2g}^x e_g^y$ ($x+y=5$) configurations in terms of Richardson parameters.

Diagonal elements $H(i,i) \equiv \langle i \rangle$.

$\langle t_{2g}^3({}^4A_{2g})e_g^2({}^3A_{2g})\text{-}{}^6A_{1g}\rangle = \frac{9}{2}\bar{J}(tt) - \frac{9}{2}\bar{K}(tt) + 6\bar{J}(et) - 6\bar{K}(et) + 2\bar{J}(ee) - 2\bar{K}(ee)$

$\langle t_{2g}^3({}^4A_{2g})e_g^2({}^1A_{1g})\text{-}{}^4A_{2g}\rangle = \frac{9}{2}\bar{J}(tt) - \frac{9}{2}\bar{K}(tt) + 6\bar{J}(et) - 3\bar{K}(et) + 2\bar{K}(ee)$

$\langle t_{2g}^3({}^4A_{2g})e_g^2({}^3A_{2g})\text{-}{}^4A_{1g}\rangle = \frac{9}{2}\bar{J}(tt) - \frac{9}{2}\bar{K}(tt) + 6\bar{J}(et) - \bar{K}(et) + 2\bar{J}(ee) - 2\bar{K}(ee)$

$\langle t_{2g}^3({}^2E_g)e_g^2({}^3A_{2g})\text{-}{}^4E_g\rangle = \frac{9}{2}\bar{J}(tt) - \frac{9}{2}\bar{K}(tt) + 3K(tt) + 6\bar{J}(et) - 4\bar{K}(et) + 2\bar{J}(ee) - 2\bar{K}(ee)$

$\langle t_{2g}^3({}^4A_{2g})e_g^2({}^1E_g)\text{-}{}^4E_g\rangle = \frac{9}{2}\bar{J}(tt) - \frac{9}{2}\bar{K}(tt) + 6\bar{J}(et) - 3\bar{K}(et) + \bar{J}(ee)$

$\langle t_{2g}^4({}^3T_{1g})e_g\text{-}{}^4T_{1g}\rangle = \frac{15}{2}\bar{J}(tt) - \frac{9}{2}\bar{K}(tt) + 3\bar{J}(et) + J(et) - 3\bar{K}(et)$

$\langle t_{2g}^3({}^2T_{2g})e_g^2({}^3A_{2g})\text{-}{}^4T_{1g}\rangle = 3\bar{J}(tt) + 6\bar{J}(et) - 4\bar{K}(et) + 2\bar{J}(ee) - 2\bar{K}(ee)$

$\langle t_{2g}^2({}^3T_{1g})e_g^3\text{-}{}^4T_{1g}\rangle = \frac{3}{2}\bar{J}(tt) - \frac{3}{2}\bar{K}(tt) + 5\bar{J}(et) + J(et) - 4\bar{K}(et) + 4\bar{J}(ee) - 2\bar{K}(ee)$

$\langle t_{2g}^4({}^3T_{1g})e_g\text{-}{}^4T_{2g}\rangle = \frac{15}{2}\bar{J}(tt) - \frac{9}{2}\bar{K}(tt) + 5\bar{J}(et) - J(et) - 3\bar{K}(et)$

$\langle t_{2g}^3({}^2T_{1g})e_g^2({}^3A_{2g})\text{-}{}^4T_{2g}\rangle = 3\bar{J}(tt) - 2K(tt) + 6\bar{J}(et) - 4\bar{K}(et) + 2\bar{J}(ee) - 2\bar{K}(ee)$

$\langle t_{2g}^2({}^3T_{1g})e_g^3\text{-}{}^4T_{2g}\rangle = \frac{3}{2}\bar{J}(tt) - \frac{3}{2}\bar{K}(tt) + 7\bar{J}(et) - J(et) - 4\bar{K}(et) + 4\bar{J}(ee) - 2\bar{K}(ee)$

Off-diagonal elements

$\langle {}^4E_g \mid \hat{\mathbf{V}} \mid {}^4E_g\rangle = \sqrt{3}[\bar{K}(et) - K(et)]$

$\langle t_{2g}^4({}^3T_{1g})e_g\text{-}{}^4T_{1g} \mid \hat{\mathbf{V}} \mid t_{2g}^3({}^2T_{2g})e_g^2({}^3A_{2g})\text{-}{}^4T_{1g}\rangle = \sqrt{6}i$

$\langle t_{2g}^4({}^3T_{1g})e_g\text{-}{}^4T_{1g} \mid \hat{\mathbf{V}} \mid t_{2g}^2({}^3T_{1g})e_g^3\text{-}{}^4T_{1g}\rangle = -2\bar{K}(et) + K(et)$

$\langle t_{2g}^3({}^2T_{2g})e_g^2({}^3A_{2g})\text{-}{}^4T_{1g} \mid \hat{\mathbf{V}} \mid t_{2g}^2({}^3T_{1g})e_g^3\text{-}{}^4T_{1g}\rangle = -\sqrt{6}i$

$\langle t_{2g}^4({}^3T_{1g})e_g\text{-}{}^4T_{2g} \mid \hat{\mathbf{V}} \mid t_{2g}^3({}^2T_{1g})e_g^2({}^3A_{2g})\text{-}{}^4T_{2g}\rangle = -\sqrt{2}i$

$\langle t_{2g}^4({}^3T_{1g})e_g\text{-}{}^4T_{2g} \mid \hat{\mathbf{V}} \mid t_{2g}^2({}^2T_{1g})e_g^3\text{-}{}^4T_{2g}\rangle = -K(et)$

$\langle t_{2g}^3({}^2T_{1g})e_g^2({}^3A_{2g})\text{-}{}^4T_{2g} \mid \hat{\mathbf{V}} \mid t_{2g}^2({}^2T_{1g})e_g^3\text{-}{}^4T_{2g}\rangle = -\sqrt{2}i$

matrix in Table III in this case) *before* diagonalization. The eigenvalues of the $\underline{H}$ (plus the CEC) matrix give rise to the CEC-corrected spectral description.[67]

To compute the cluster CEC matrix we then need the free-ion CEC matrix and the vector coupling coefficients. The free-ion CEC matrix has been found from the observed spectrum of the Mn^{2+} ion[68,69] and the free-ion electronic transition energies $E(iSL) - E(0SL)$ computed with the 2-ζ $3d$ function of Ref. 61. This matrix appears in the first row of Table IV. The required $\langle iSL \mid t_{2g}^x e_g^y - jS\Gamma\rangle$ coefficients have been computed by diagonalizing the free-ion Hamiltonian in the

TABLE IV. Atomic CEC for Mn^{2+}, $\langle iSL \mid t_{2g}^x e_g^y jS\Gamma\rangle$ coefficients and $\langle \text{MO } t_{2g} \mid \text{AO } 3dt_{2g}\rangle$ and $\langle \text{MO } e_g \mid \text{AO } 3de_g\rangle$ overlap integrals.

				Mn^{2+}:^6S			
		^4G		^4P	^4D		^4F
CEC (iSL) cm^{-1}		−4383		−6810	−6584		−8915
$\langle iSL \mid t_{2g}^x e_g^y jS\Gamma\rangle$ coefficients							
$^4T_{1g}$	1[a]	2	3	$^4T_{2g}$	1	2	3
^4G	0.707 106 78	0.0	0.707 106 78	^4G	0.462 910 05	0.755 928 95	0.462 910 05
^4P	−0.632 455 54	0.447 213 58	0.632 455 54	^4D	−0.534 522 49	0.654 653 67	−0.534 522 49
^4F	0.316 227 76	0.894 427 20	−0.316 227 76	^4F	0.707 106 78	0.0	−0.707 106 78

^4E_g	1	2	$^4A_{1g}$ 1	$^4A_{2g}$ 1
^4G	0.755 928 94	0.654 653 68	^4G 1	^4F 1
^4D	0.654 653 68	−0.755 928 94		

	R(Mn-F) a.u.							
	3.0	3.2	3.4	3.6	3.8	4.0	4.2	4.4
$\langle \text{MO } t_{2g} \mid \text{AO } 3d\ t_{2g}\rangle$	0.9345	0.9553	0.9696	0.9795	0.9863	0.9909	0.9939	0.9960
$\langle \text{MO } e_g \mid \text{AO } 3d\ e_g\rangle$	0.8619	0.8857	0.9058	0.9227	0.9369	0.9488	0.9586	0.9669

[a]Labels 1, 2, 3 for the $\mid t_{2g}^x e_g^y - jS\Gamma\rangle$ vectors correspond to those in Ref. 64. CEC matrices obtained with these coefficients have the phase of the CI matrices in Ref. 64.

$|t_{2g}^{x}e_g^{y}-jS\Gamma\rangle$ basis. They are also collected in Table IV.

As in earlier studies,[54,67] we can assume that the $|t_{2g}^{x}e_g^{y}-jS\Gamma\rangle$ basis is formed of pure-d AO's. In this case the cluster CEC is an empirical correction independent of the metal-ligand distance. For that reason we can call it rigid or not delocalized CEC and write CECr for this type of correction. On the other hand, some degree of electronic delocalization can be included in the CEC if the $S\Gamma$ basis is assumed to be made of MO's, as it is in the case of the Hartree-Fock description. To first-order such delocalization can be easily incorporated through the action of the overlap integrals $\langle \mathrm{MO}t_{2g} \mid \mathrm{AO}3dt_{2g}\rangle$ and $\langle \mathrm{MO}e_g \mid \mathrm{AO}3de_g\rangle$.[67] We will use the label CECd for this partially delocalized CEC. The CECd matrix depends on the atomic basis set (as the CECr does), the metal-ligand distance, and the characteristics of the SCF solution, due to the presence of the $\langle \mathrm{MO} \mid \mathrm{AO}\rangle$ overlap integrals. These integrals, computed with the SCF SPDDSP solutions of the $t_{2g}^{3}e_g^{2}$-$^6A_{1g}$ state at eight values of R are collected in Table IV.

D. Cluster-lattice interaction

This interaction has been represented by the one-electron operator $\hat{\mathbf{V}}_{\mathrm{ext}}$ appearing in the Fock operator of the cluster.[49] We will discuss the MnF_6^{4-} system in $RbMnF_3$. In order to study the interaction we will examine three types of SCF calculations:

(i) MnF_6^{4-} *in vacuo*. In this calculation $\hat{\mathbf{V}}_{\mathrm{ext}}$ is taken to be zero.

(ii) Unrelaxed lattice (UL) description. $\hat{\mathbf{V}}_{\mathrm{ext}}$ is computed from the lattice potential (Ewald method) generated by a rigid, unrelaxed point-charge representation of the $RbMnF_3$.[56]

(iii) Charge-relaxed lattice (CRL) model. The point charges representing the ions in $RbMnF_3$ are relaxed from their nominal values and made consistent with the electronic charges deduced from the SCF calculation on the MnF_6^{4-} cluster.[57] This procedure was applied to the CrF_6^{3-} ion in CrF_3 (Ref. 58), and it seems to be appropriate for shared-cluster lattices such as the $RbMnF_3$.

III. VERTICAL *d-d* SPECTRUM AND SPECTRAL PARAMETERS

A. Wave functions

Here we present results of the SCF-MO wave function of MnF_6^{4-} that are appropriate for discussing the *d-d* spectrum, i.e., those related to the valence e_g and t_{2g} MO's. In Table V we collect the MO coefficients from the ground-state SPDD solution of the MnF_6^{4-} *in vacuo*, at the typical $R=4.00$ a.u. (2.12 Å). SPDDSP results are also collected in this Table in order to show the influence of the $4s$ and $4p$ functions. The last column of Table V contains the SPDDSP solution corresponding to the MnF_6^{4-} in the lattice of $RbMnF_3$, UL model. The relaxed-lattice description is too similar to the UL one to deserve tabulation.

From Table V we observe the small effects of the empty $4s$ and $4p$ AO's in the composition of the e_g and t_{2g} MO's. Lattice effects in these orbitals are also too small to have physical significance.

The composition of the open-shell $3e_g$ and $2t_{2g}$ MO's reveals a slight $3d$ expansion in the second MO and a still smaller compression in the $3e_g$ according to the signs of the $3d_M$ and $3d_I$ basis functions. These open-shell MO's also reveal that the π bonding in MnF_6^{4-} (t_{2g} MO's) is

TABLE V. SCF-MO coefficients of the e_g and t_{2g} MO's corresponding to three different solutions of the $^6A_{1g}$ state of MnF_6^{4-} at $R=4.0$ a.u.

MO	Basis	SPDD *in vacuo*	SPDDSP *in vacuo*	SPDDSP plus lattice, UL
$1e_g$	$3d_M$	0.0322	0.0257	0.0260
	$3d_I$	−0.0092	−0.0082	−0.0083
	χ_s	0.9960	0.9968	0.9966
	χ_σ	0.0095	−0.0196	−0.0272
$2e_g$		0.2961	0.2552	0.2565
		−0.0970	−0.0966	−0.0965
		−0.0515	−0.0156	−0.0084
		0.9413	0.9541	0.9536
$3e_g$		−0.9889	−0.9977	−0.9964
		−0.0033	−0.0022	−0.0034
		0.1334	0.1347	0.1360
		0.3296	0.2901	0.2911
$1t_{2g}$	$3d_M$	0.1658	0.1253	0.1276
	$3d_I$	−0.0611	−0.0539	−0.0541
	χ_π	0.9843	0.9899	0.9896
$2t_{2g}$		−1.0288	−1.0352	−1.0341
		0.0398	0.0435	0.0424
		0.1690	0.1351	0.1371

TABLE VI. t_{2g}-e_g electron-repulsion integrals (cm^{-1}) and orbital energies (a.u.) of the open-shell $3e_g$ and $2t_{2g}$ MO's for different solutions of the $^6A_{1g}$ at $R=4.0$ a.u.

Parameter	SPDDSP *in vacuo*	SPDDSP plus lattice, UL	Free ion
$\bar{J}(tt)$	175 394	175 418	181 334
$\bar{K}(tt)$	66 317	66 326	68 608
$K(tt)$	7067	7068	7347
$\bar{J}(et)$	173 362	173 370	178 639
$\bar{K}(et)$	6019	6018	6246
$J(et)$	169 087	169 093	174 233
$K(et)$	8142	8141	8449
$\bar{J}(ee)$	178 020	178 010	182 681
$\bar{K}(ee)$	97 219	97 213	99 789
i	1837	1837	1908
Orbital energies	SPDDSP *in vacuo*	SPDDSP plus lattice, UL	
$\epsilon(3e_g)$	0.444 82	−0.293 73	
$\epsilon(2t_{2g})$	0.401 97	−0.336 86	

noticeably smaller than the σ bonding (e_g MO's). The $2p\sigma$ ligand orbitals are the most efficient channels for the ligand—to—metal-atom charge transfer. This characteristic of the $2p\sigma$ orbital was also found in NiF_6^{4-}.[51]

From the SCF wave function we compute the ten independent t_{2g}-e_g electronic repulsion integrals defined in Table II. With the orbital energies $\epsilon(3e_g)$ and $\epsilon(2t_{2g})$, these integrals are the raw material for the spectral calculations described below. In Table VI we give their SPDDSP values, corresponding to cluster—*in-vacuo* and cluster—in-the-lattice calculations, as well as their free-ion limits. In this table we also present the $3e_g$ and $2t_{2g}$ orbital energies. They are positive in the cluster—*in-vacuo* calculation, but the cluster-lattice interaction reduces their value by about 3.5 eV *per* $3d$ electron, making them negative. This satisfactory result was also found in K_2NaCrF_6 and CrF_3.[58] Finally, we notice that although the presence of the $4s$ and $4p$ AO's gives rise to noticeable increases in $\epsilon(3e_g)$ and $\epsilon(2t_{2g})$, $\Delta\epsilon=\epsilon(3e_g)-\epsilon(2t_{2g})$ remains almost unchanged [$\Delta\epsilon$(SPDD)=1.4 eV, $\Delta\epsilon$(SPDDSP)=1.2 eV]. The effect of the cluster-lattice interaction on $\Delta\epsilon$ is negligible.

B. Single-excitation transitions

Although we have calculated the electronic energies of the MnF_6^{4-} at eight values of R, we will discuss here the vertical electronic transitions at $R=4.0$ a.u., a distance very close to that observed in $RbMnF_3$, $R_e=4.006$ a.u.[70] We present results deduced from the SPDDSP SCF calculation on the ground state. MO's obtained from excited states within the d^5 configuration give an entirely comparable image. For instance, the values of the high-energy transitions computed with the solution of the $t_{2g}^3e_g^2$-$^4A_{1g}$ differ from those obtained with the ground-state solution by, at most, 1 kK. Relaxation energies computed within the $t_{2g}^3e_g^2$ configuration are smaller than 500 cm^{-1} and do not alter this discussion. The effects of the cluster-lattice interaction on these transitions are also uniformly small. As a matter of fact, they are comparable to or smaller than those due to modifications in the core-valence partition. We will refer later to such effects. Let us see now the results of the SPDDSP cluster—*in-vacuo* calculations.

In Table VII we have collected the single-excitation transitions observed in $RbMnF_3$ at room and liquid-nitrogen temperatures by Mehra and Venkateswarlu,[25] as well as our different theoretical results. The room-temperature spectrum of $RbMnF_3$ has also been given by Stevenson[7] and Ferguson.[9] As stated in the Introduction, the spectrum of MnF_6^{4-} has been measured many times in a number of crystals but the single electronic transitions generally differ from those given in Ref. 25 and collected in Table VII by less than 300 cm^{-1}. This conspicuous feature of the spectra of MnF_6^{4-} suggests that the sextet-quartet electronic transitions of this system are mainly determined by the components of the cluster. That is, they are in agreement with the results of our calculations on the cluster-lattice interaction.

The third column of Table VII contains our first-order results. The overall calculation is rather poor, giving a rms deviation larger than 8 kK and the wrong order for the $^4A_{1g}$,$^4T_{2g}^a$ and the $^4A_{2g}$,$^4T_{1g}^c$ states. Configuration interaction limited to the $t_{2g}^xe_g^y$ ($x+y=5$) configurations represents an improvement of about 2 kK in the rms deviation. Now the order of the computed multiplets is in qualitative agreement with the experiment, but the spectral representation is still poor. Inclusion of the CECr is clearly a significant improvement over the previous calculation. The rms deviation is now only 1.2 kK. The delocalization reduces the values of the CECr matrix elements and gives rise to a softer correction, the CECd. Since our nonempirical results give a computed spectrum too high with respect to the observed values, this property of the CECd makes it less efficient than the CECr. This behavior of the CEC was also observed in CrF_6^{3-} and NiF_6^{4-} (Ref. 67), but in CrF_6^{4-} (Refs. 54 and 63) the

TABLE VII. Observed and calculated spectrum of MnF_6^{4-} in $RbMnF_3$. Note, calculated values have been obtained from the SPDDSP-SCF solution of the ground state, cluster—*in-vacuo* calculation at $R = 4.00$ a.u. Numbers in kK.

Transition	Observed in $RbMnF_3$[a] 300 K	77 K	Calculated in this work Diagonal	CI	CI plus CECr	CI plus CECd
$^4T_{1g}^a$	19.286	19.150	23.95	22.67	17.28	18.17
$^4T_{2g}^a$	23.282	23.106	32.50	27.65	22.38	23.32
$^4E_g^a$	25.151	25.195	33.24	30.13	25.75	26.77
	25.278	25.336				
$^4A_{1g}$	25.484	25.543	30.10	30.10	25.71	26.74
	25.700	25.759				
$^4T_{2g}^b$	28.362	27.917	33.24	35.12	28.78	30.13
		28.129				
		28.258				
		28.385				
$^4E_g^b$	30.067	30.140	34.48	37.59	31.00	32.54
	30.395	30.478				
$^4T_{1g}^b$	32.414	32.446	47.38	41.07	34.80	36.47
$^4A_{2g}$	41.152	41.158	50.89	50.89	41.98	44.06
$^4T_{1g}^c$		41.926[b]	44.26	51.84	43.40	45.49
$^4T_{2g}^c$	44.249[b]	43.914[b]	52.81	55.79	47.52	49.82
rms deviation			8.4	6.6	1.2	2.2

[a]Reference 25.

[b]These peaks can be double-excitations transitions.

CECd turned out to be more efficient.

It is difficult to see why the CECr works better than the CECd which, in principle, is a more adequate correction. It appears that inclusion of delocalization effects in the CECr by means of the $\langle MO \mid AO \rangle$ integrals[67] overemphasizes the delocalization, suggesting that the multicenter pure-ligand and metal-ligand contributions to these effects could be important. In any case, calculations including any type of CEC give a rather good representation of the overall sextet-quartet spectrum.

In the best calculation, the first $^4T_{1g}$ and $^4T_{2g}$ states remain somewhat lower than the observed bands. This effect is not due to an overcorrection on the part of the CEC but to the large theoretical value of $10Dq$ which turns out to be some 2 kK larger than the observed value (see below). This result decreases the lower quartets, which have negative slope with respect to $10Dq$, and increases the higher ones, with positive slopes. A vertical calculation at a value of R slightly larger than 4.0 a.u. would have corrected both difficulties. For that reason it is satisfactory to see that in our best calculations the $10Dq$-independent (or near independent) transitions are very well reproduced.

C. Double-excitation transitions

In the crystal-field interpretation of the high-energy bands (above 35 kK) of the spectra of Mn^{2+} in fluorides several difficulties are encountered. First, the band energies differ from the theoretical values by amounts larger than those found in the lower energy part of the spectrum. Second, the high-energy bands are more intense than expected. Third, these bands shift to lower energies upon cooling, in contrast with the crystal-field prediction (these bands are increasing functions of $10Dq$, that in turn should increase upon cooling). Furthermore, the widths of these bands are very similar to the values found in the lower-energy bands. All these difficulties are essentially removed if the absorptions are interpreted as double excitations corresponding to the simultaneous optical excitation of two neighboring magnetic ions. This type of transition has been discussed in different systems containing the MnF_6^{4-} ion: Mn^{2+}:$KZnF_3$,[17,18] $KMnF_3$,[17,19,27] $KZn_{1-x-y}Mn_xNi_yF_3$, and $KMn_xNi_{1-x}F_3$,[34] $RbMnF_3$,[9,14,19] $NaMnF_3$,[27] and MnF_2,[8,9,13,14] among others. More recently such transitions have been observed in $BaMnF_4$,[30] and in Mn^{2+}:LiF and Mn^{2+}:NaF.[39] The double excitation bands show very slight changes from crystal to crystal, in accordance with the behavior of the low-energy bands, the only exception being the $^4T_{1g}^a + {}^4A_{1g}, {}^4E_g^a$ and the $^4T_{2g}^a + {}^4A_{1g}, {}^4E_g^a$ peaks observed in the as-grown Mn^{2+}:LiF crystal.[39] In this case the bands appear 3—4 kK below their expected positions, a result probably due to a strong inwards relaxation of the fluoride ions.[39]

In Table VIII we collect the double excitation bands observed in $RbMnF_3$, as well as our computed values. The transitions reported by Mehra and Venkateswarlu[25] were not assigned by these authors to double excitations but the work of Srivastava and Mehra on $NaMnF_3$,[27] and the measurements of Stokowski, Sell, and Guggenheim,[14] strongly suggest such assignment.

The theoretical results in Table VIII are similar to those on the single excitations in Table VII. Again, CI improves the diagonal spectrum (now by 4 kK in the rms deviation) and the CEC brings the theoretical spectrum into

TABLE VIII. Observed and calculated double-excitation transitions in $RbMnF_3$. Note, calculated values from the SPDDSP-SCF solution of the ground state, cluster—*in-vacuo* calculation at $R = 4.00$ a.u. Numbers in kK.

Transition	Observed		Calculated			
$^6A_{1g}+{}^6A_{1g}$	Ref. 25	Ref. 9	Ref. 14	Diagonal	CI	CI plus CECr	CI plus CECd
$^4T_{1g}^a+{}^4T_{1g}^a$	38.31[a]	38.31 (20 K)	38.3	47.9	45.3	34.6	36.3
$^4T_{1g}^a+{}^4T_{2g}^a$	41.926	42.19 (20 K)	42.2	56.5	50.3	39.7	41.5
$^4T_{1g}^a+{}^4A_{1g},{}^4E_g^a$	43.914	44.20 (300 K)	43.9,44.2	57.3,54.1	52.8	43.0	44.9
$^4T_{2g}^a+{}^4T_{2g}^a$			46.7	65.0	55.3	44.8	46.6
$^4T_{1g}^a+{}^4T_{2g}^b$			47.3, 47.8	57.2	57.8	46.1	48.3
$^4T_{2g}^a+{}^4A_{1g},{}^4E_g^a$			48.4, 48.9	65.7,62.6	57.8	48.1	50.1
$^4T_{1g}^a+{}^4E_g^b$			49.2	58.4	60.3	48.3	50.7
$^4A_{1g},{}^4E_g+{}^4A_{1g},{}^4E_g$			50.8	63.3	60.2	51.5	53.5
rms deviation				13.4	9.2	1.9	1.5

[a]Quoted by Srivastava and Mehra, Ref. 27.

a close agreement with the observations of Stokowski *et al.*[14] It is interesting to see that the CECd works now a little better than the CECr. This difference with the results on single-excitation transitions comes from the slight separation of the observed double excitations from the simple sum of the two single peaks involved in them. Such separations, of about 0.5 kK, can be due to exchange interactions or to lattice distorsion effects, depending perhaps on the symmetry of the excited state.[14]

Results of Table VIII also give further support to the assignment of the peaks at 41.93 and 43.91 kK (Ref. 25) to double excitation transitions, more than to the $^6A_{1g}\rightarrow{}^4T_{1g}^c,{}^4T_{2g}^c$ single excitations. When assigned to single excitations, these two peaks give deviations larger than the rms of the corresponding calculation. In the CECr calculation, the $^4T_{1g}^c$ deviates 1.5 kK from 41.93, and the $^4T_{2g}^c$ deviates 3.6 kK from 43.91. However, if assigned to double excitations, we find the $^4T_{1g}^a+{}^4T_{2g}^a$ at 39.6 and the $^4T_{1g}^a+{}^4A_{1g},{}^4E_g^a$ at 43.0 kK, with deviations of 2.3 kK and 0.9 kK, respectively. The effect is particularly clear in the best calculation: The assignments to single excitation give deviations for the $^4T_{1g}^c$ and $^4T_{2g}^c$ of 3.6 kK and 5.9 kK, respectively, but the assignment to double excitation gives the $^4T_{1g}^a+{}^4T_{2g}^a$ at 41.4 and the $^4T_{1g}^a+{}^4A_{1g},{}^4E_g^a$ at 44.9, with deviations more than three times smaller than those found in the assignment to single excitations. This inference from the theoretical results is analogous to that deducible from the crystal-field analysis of the spectrum and reinforces the (strong) arguments already known[9,14,30] in favor of the assignment to double excitations. A calculation of the transition intensity of these bands will give important information on this assignment. As stated in the Introduction, we have not attempted such calculation in this paper.

D. Lattice potential effects on the calculated spectrum

In Table IX we present the results of two spectral calculations including the potential of the lattice of $RbMnF_3$. For brevity we collect only the results of the best calculations, i.e., those including the CEC correction. We can see that the effects of the lattice potential considered here are negligible. Indeed, such effects are smaller than the changes produced by changes in the core-valence partition, which are less than 1 kK, as can be seen by comparing Tables VII and IX. This result suggests that in concentrated materials, such as the perovskite considered here, the optical spectrum is mainly determined by the components of the MnF_6^{4-} cluster. This is also in agreement with the negligible differences observed in the spectra of the perovskite fluorides and in MnF_2. In other materials, where ligand relaxations (induced by charge compensation and other factors) occur, the situation could be rather different, as in the case of Mn^{2+}:LiF,[39] already mentioned.

E. Theoretical crystal-field parameters

Here we present the crystal-field parameters deduced from our *computed* spectrum. In this way, the information obtained from the SCF results is particularly suitable for comparison with both empirical crystal-field analyses

TABLE IX. Computed single-excitation transitions including the lattice potential of $RbMnF_3$. Note, SPDD results of the ground state at $R = 4.00$ a.u. Numbers in kK.

	CI plus CECr			CI plus CECd		
Transition	*in vacuo*[a]	UL[b]	CRL[c]	*in vacuo*	UL	CRL
$^4T_{1g}^a$	16.4	16.6	16.6	17.6	17.7	17.8
$^4T_{2g}^a$	21.6	21.7	21.8	22.8	22.9	23.0
$^4E_g^a$	25.2	25.2	25.3	26.5	26.5	26.5
$^4A_{1g}$	25.0	25.1	25.1	26.3	26.4	26.4
$^4T_{2g}^b$	28.2	28.2	28.2	29.9	29.9	29.9
$^4E_g^b$	30.2	30.3	30.3	32.2	32.2	32.2
$^4T_{1g}^b$	34.3	34.3	34.3	36.4	36.4	36.4
$^4A_{2g}$	40.7	40.9	40.9	43.3	43.5	43.5
$^4T_{1g}^c$	42.7	42.7	42.8	45.3	45.3	45.3
$^4T_{2g}^c$	46.8	46.8	46.8	49.7	49.6	49.6

[a]Cluster—*in-vacuo* calculation.
[b]Unrelaxed-lattice calculation.
[c]Charge-relaxed-lattice calculation.

and nonempirical calculations. We have used the SPDDSP results corresponding to the SCF solution of the ground state at $R = 4.00$ a.u., as above. From the above discussion of the lattice effects on the computed electronic transitions, we expect negligible differences in the values of the crystal-field parameters obtained with and without inclusion of the lattice potential. This is, indeed, the case, and we will limit the following discussion to the results deduced from the cluster—*in-vacuo* calculation.

Crystal-field analyses are currently performed in terms of the familiar Racah parameters B and C, and the d-splitting parameter Δ or $10Dq$. If the $\alpha L(L+1)$ correction of Trees and Racah[71] is included, α is also considered as an adjustable parameter. On the other hand, Sharma *et al.*[65] have emphasized the convenience of using the set of ten independent repulsion integrals,[64] plus Δ, as fitting parameters. This procedure will enlarge our knowledge of several Coulomb and exchange interactions in transition-metal systems. The method requires, however, a larger amount of experimental data. Sharma and Sundaram[66] have analyzed the excitation spectrum of an electron-irradiated Mn^{2+}:MgF_2 crystal reported by Yun *et al.*,[36] and have given the best values of the ten integrals and $10Dq$. These parameters were computed by solving the inverse eigenvalue problem of the electrostatic interaction matrices for the quartet and doublet states of the d^5 configuration. This set of empirical parameters constitute an interesting test for the Coulomb and exchange interactions computed in this work from the HFR wave function of MnF_6^{4-}. For that reason we have collected them in Table X, their equivalent expressions in terms of the parameters of Richardson *et al.*[49] used in this work and our theoretical results corresponding to different calculations. All our numbers come from the SPDDSP SCF solution of the ground state and have been obtained by means of the systematic linearization[59,60] of the electrostatic matrices of the quartets.

In considering these parameters we would like to remark on the differences between the method of calculation of Sharma and Sundaram[66] and ours: They obtain the parameters by adjusting the electrostatic matrices to the *observed* spectrum of Mn^{2+}:MgF_2,[36] we do adjust the matrices to the *computed* spectrum of the MnF_6^{4-} unit *in vacuo*. Furthermore, in the computed spectrum we have considered only sextet-quartet transitions.

Since the first-order or diagonal calculation involves a linear relation between the transition energies and the spectral parameters, our first-order set in Table X exactly coincides with the numbers in Table VI. As discussed above, this set gives a rms deviation of 8.4 kK (Table VII) with the observed spectrum of $RbMnF_3$. Since this spectrum is not very different from that of Mn^{2+}:MgF_2 used by Sharma and Sundaram,[66] their parameters and ours should show noticeable differences. Our computed spectrum is still poor after CI (rms deviation of 6.6 kK, Table VII) and indeed the corresponding parameters are quite similar to the diagonal set. On the other hand, the CI plus the CECr calculation gives a theoretical spectrum quite good and the corresponding parameters closely resemble those given by Sharma and Sundaram,[66] as it can be seen in Table X. Only small differences appear between the two sets, except for $10Dq$ and V_7, which is a $3e_g$-$2t_{2g}$ exchange integral. These differences can be associated to the action of the doublet states considered in Ref. 66, and to differences in the mathematical procedures employed. In general, the consistency between the set of Sharma and Sundaram and ours is quite remarkable.

A few works can be said about the information that our parameters can give on the spectrum of Mn^{2+}:MgF_2.[36] The feature at 20 833 cm^{-1} is assigned by Yun *et al.*[36] to the $^4T_{1g}(^4G)$. Its separation from the peak at 19 153, 1680 cm^{-1}, is probably too big to be due to the spin-orbit splitting of this quartet. Sharma and Sundaram[66] assign this feature to the $^4T_{2g}(^4G)$. Our parameters locate the $^4T_{2g}(^4G)$ at 22 380 cm^{-1}, and it is observed in many systems at this frequency. Therefore, the assignment of this feature appears somewhat uncertain. The sixth peak, ob-

served at 35088 cm^{-1}, is assigned to the $^2T_{2g}(^2D)$ doublet in Ref. 66. Our calculation locates the $^4T_{1g}(^4P)$, proposed by Yun *et al.*,[36] at 34800 cm^{-1}. The peak at 40000 cm^{-1} is assigned to the $^2A_{1g}(^2G)$, and that at 43554 cm^{-1} to the $^4T_{1g}(^4F)$.[66] The latter assignment agrees quite well with our calculation (43400 cm^{-1}).

In spite of the clear advantages of the ten-parameter set, it is still convenient to analyze the optical spectrum in terms of the classical B and C parameters. As a matter of fact, a *very good agreement* can be reached with this simple scheme, as we show below.

Again, we have obtained these parameters by means of the linearization analysis of the electrostatic matrices.[59,60] This seems to be an appropriate method of obtaining a theoretical estimation of $10Dq$ from the values of differences in *total* energies, since in the d^5 configuration there is not a transition energy that gives directly $10Dq$. Although some authors have questioned the convenience of using the Racah-Trees correction[71] in the calculation of the best parameters, we have introduced it in order to compare our results with those of Mehra and Venkateswarlu.[25] We present two calculations. In the first one the Racah-Trees constant α is fixed to its free-ion value, usually accepted as 76 cm^{-1}. In the second calculation α is considered as an adjustable parameter. In both calculations we deal with the calculated spectrum after CI and after CI plus the CECr. For comparison, we deal also with the observed transitions.[25] In all cases we used the spectral assignment of Table VII. The double excitation transitions have not been included in the calculation. The results appear in Table XI.

Several interesting points can be noticed from these results. First, we see that the CEC reduces the values of B and C, in both calculations, by about 18%. $10Dq$, however, is changed only some 2% by the inclusion of this correction. This result confirms that the CEC corrects mainly the correlation error, and, consequently, reduces the electronic repulsion. After CEC the theoretical B and C are very close to the experimental values but $10Dq$ remains about 2 kK high. This discrepancy in $10Dq$ is a manifestation of the deviation theory experiment in the present calculation and explains the deviations in Table VII. The calculations with α variable produce, for the observed and CEC spectra, crystal-field parameters very similar to those found when $\alpha = 76$ cm^{-1}. However, the CI spectrum gives a noticeable separation, revealing that it is a rather different spectrum. Also, we notice that the ten-parameter scheme (Table X) gives a $10Dq$ 1 kK larger than the value found with the three-parameter scheme. Sharma and Sundaram[66] find a $10Dq$ of 5.7 kK, which is 2 kK lower than the value given in Ref. 25 (7.8 kK).

Compared with other theoretical calculations of $10Dq$, our discrepancy is slightly larger than that found by Adachi *et al.*[46] in their discrete variational $X\alpha$ calculation on $KMnF_3$. Their value of $10Dq$, defined as the difference between the spin-up e_g and t_{2g} orbital energies, turns out to be 6.7 kK. The HF-SCF calculations of Matsuoka[42] on MnF_6^{4-} over Gaussian-type orbitals (GTO's) gave values for $10Dq$ from 5.0 kK to 6.0 kK, depending upon the different approximations involved.

TABLE X. Spectral parameters (cm^{-1}) given by Sharma and Sundaram (Ref. 66) and different sets computed in this work.

Sharma's parameters[a]	Equivalent expressions (Ref. 49)	MgF_2:Mn^{2+} [b]	SPDDSP $^6A_{1g}$ *in vacuo* Diagonal	CI	CI + CECr
V_1-V_2	$-\frac{3}{2}\bar{J}_{tt}+\frac{9}{2}\bar{K}_{tt}-3K_{tt}$	11176	14135	14130	11850
V_1-V_4	$3\bar{K}_{tt}-2K_{tt}-\frac{1}{2}\bar{J}_{et}-\frac{1}{2}J_{et}$	11931	13593	13600	12090
V_1-V_5	$3\bar{K}_{tt}-2K_{tt}-\frac{1}{2}\bar{J}_{ee}-\bar{K}_{ee}$	647	−1411	−1410	890
V_3	$\frac{\sqrt{3}}{2}\bar{J}_{et}-\frac{\sqrt{3}}{2}J_{et}$	2469	3703	3710	3090
V_6	$-\frac{1}{2}\bar{J}_{ee}+\bar{K}_{ee}$	6026	8209	8210	6790
V_7	$\frac{3}{2}\bar{K}_{et}-\frac{1}{2}K_{et}$	2725	4958	4960	4140
V_8	$-\frac{\sqrt{3}}{2}\bar{K}_{et}+\frac{\sqrt{3}}{2}K_{et}$	1584	1839	1840	1530
V_9	i	2164	1837	1840	1540
V_{10}	K_{tt}	6093	7067	7070	5930
Dq		571	769	769	1126

[a]Reference 65.
[b]Reference 66.

TABLE XI. Best crystal-field parameters (cm^{-1}) deduced from the observed ($RbMnF_3$, 77 K) and calculated spectra of MnF_6^{4-}.

	$\alpha=76$ cm^{-1}			α variable		
Parameter	Expt.[a]	CI	CI plus CECr	Expt.[b]	CI	CI plus CECr
$10Dq$	7800	10389	10074	7603	10126	10063
B	840	1097	888	859	1065	886
C	3080	3654	3072	3005	3906	3087
C/B	3.67	3.33	3.46	3.50	3.67	3.48
α	76	76	76	80	−2	71
rms deviation	232	378	67	176	73	64

[a]Given by Mehra and Venkateswarlu (Ref. 25).
[b]Obtained in this work from the data in Ref. 25.

IV. R DEPENDENCE OF THE COMPUTED SINGLE-EXCITATION TRANSITIONS AND THE THEORETICAL SPECTRAL PARAMETERS

In Fig. 1 we present the ten electronic transitions of the d^5 configuration, computed from $R=3.0$ a.u. (1.59 Å) to $R=4.4$ a.u. (2.33 Å) with the cluster—*in-vacuo* SPDDSP solutions of the ground state, after inclusion of the CI and the CECr corrections. Three types of transitions can be distinguished in this figure:

(a) Those involving an excited state of the $t_{2g}^4e_g$ configuration; they correspond to $e_g\rightarrow t_{2g}$ excitations, and in crystal-field theory they are decreasing functions of $10Dq$. In Fig. 1 we see that they increase with R.

(b) Intraconfigurational transitions, $t_{2g}^3e_g^2$-$^6A_{1g}\rightarrow t_{2g}^3e_g^2$-$^4\Gamma$, corresponding to spin flips within the e_g and/or t_{2g} orbitals; they are independent of $10Dq$ in (first-order) crystal-field theory. Here they show a negligible variation with R.

(c) Transitions to excited states of the $t_{2g}^2e_g^3$ configuration, involving a $t_{2g}\rightarrow e_g$ excitation; they are increasing functions of $10Dq$ in crystal-field theory, and decreasing functions of R, as Fig. 1 shows. This behavior is essentially determined by the monoelectronic contribution of the transition energy.

The results shown in Fig. 1 can be connected with the band shifts observed upon cooling the sample if we accept that these shifts are mainly due to contractions of the cluster unit. For instance, Mehra and Venkateswarlu[25] found that the $^6A_{1g}\rightarrow{}^4T_{1g}^a$, $^4T_{2g}^a$ transitions of $RbMnF_3$ show red shifts of 0.136 kK and 0.176 kK, respectively, upon cooling from 298 to 77 K. Moreover, the $^6A_{1g}\rightarrow{}^4A_{1g}$, $^4E_g^a$, $^4T_{2g}^b$, $^4E_g^b$, $^4T_{1g}^b$, $^4A_{2g}$ transitions show blue shifts about five times smaller.[25] These observations are readily understood in terms of the R dependence of these bands, shown in Fig. 1. Furthermore, the peak at 44.25 kK (298 K) shows a red shift of 0.335 kK upon cooling to 77 K,[25] in contradiction with the R dependence of the

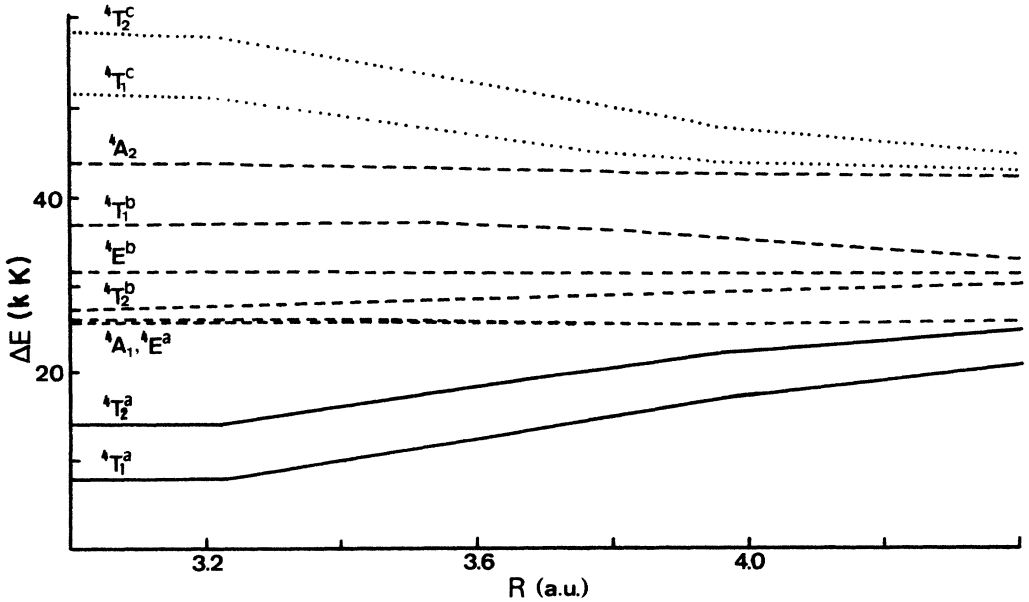

FIG. 1. Single excitation transitions of MnF_6^{4-} as functions of the internuclear distance, computed with the SPDDSP solutions of the ground state. CI + CECr calculation. Solid, dashed, and dotted lines are used for the $t_{2g}^4e_g$, $t_{2g}^3e_g^2$, and $t_{2g}^2e_g^3$ configurations, respectively.

$^4T_{2g}^c$ state, that should experience blue shifts. This red shift strongly supports the assignment of this peak to the double excitation $^6A_{1g}+{}^6A_{1g}\rightarrow{}^4T_{1g}^a+{}^4A_{1g},{}^4E_g^a$ (Table VIII).

The fitting of the $10Dq$, B, C, and α parameters to the computed spectrum, discussed in Sec. III E for $R=4.0$ a.u., is extended now to the range 3.0 a.u. $\leq R \leq 4.4$ a.u. Results from the CI and CI plus CECr calculations are shown in Fig. 2. In these calculations α turns out to be nearly independent of R. This parameter is essentially zero in the CI calculation; in the CI plus CECr case we find $\alpha=78\pm8$ cm^{-1}.

In Fig. 2 we observe, first, that $10Dq$ is very insensitive to the action of the CECr correction, in all the range of R studied here. This parameter shows a uniform variation with R, that can be represented by the inverse-power law $10Dq=CR^{-n}$, giving $n=3.60$ for 3.2 a.u. $\leq R \leq 4.4$ a.u.[72] This variation agrees with that found by Adachi *et al.*,[46] $n=3.4$, and it can be compared with the experiments. Using the linear thermal expansion coefficient at room temperature $\alpha=16.5\times10^{-6}$ K^{-1},[73,74] $R_0=2.12$ Å,[70] and the observations of Mehra and Venkateswarlu[25] on the shift of the $10Dq$, 7.60 kK at 300 K to 7.80 at 77 K, we find that $\partial(10Dq)/\partial R\simeq-26$ kK/Å. On the other hand, our SPDDSP calculations, after CI plus CECr, give $10Dq=10.063$ kK at $R=2.117$ Å and 12.326 kK at $R=2.011$ Å, predicting a variation of $10Dq$ with R of about -21 kK/Å. These two numbers are in reasonable agreement, in view of all the approximations involved, and suggest that the blue shift shown by $10Dq$ upon cooling could be due mainly to changes in the cluster size.

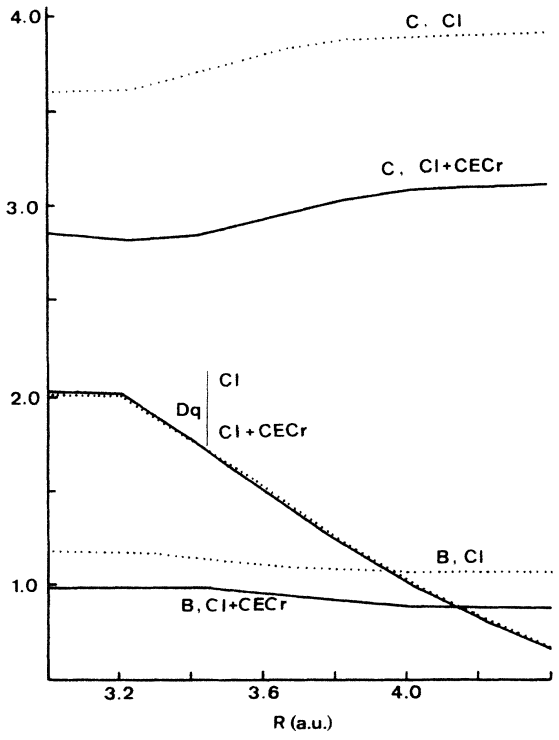

FIG. 2. Dq, B, and C parameters (in kK) deduced from the computed SPDDSP spectra after CI (dotted lines) and after CECr (solid lines) by linearization of the strong-field matrices, including the Racah-Trees correction.

The Racah parameters are very sensitive to the action of the CECr correction, in the range of R shown in Fig. 2. It is interesting to notice that B decreases slightly when R increases, whereas C shows the opposite trend. This result represents a problem if one is interested in estimating the changes in covalency with R, for a given system, by means of the Racah parameters. Their slight (and opposite) variation with R does not agree with the trends of the electronic delocalization, as measured through the SCF coefficients of the MO's. This effect was also observed in CrF_6^{4-},[54,63] where the variation of the Racah parameters with R is still smaller. The near independence of the intraconfigurational transitions (governed mainly by the repulsion integrals) with R is quite compatible with the slight R dependence of B and C. For that reason, whereas a noticeable change in the observed position of an interconfigurational band could be taken as an indication of a ligand relaxation, a change in an intraconfigurational transition seems to be a more doubtful evidence, according to the present calculations.

Let us now examine the question of the relative position of the $^4E_g^a,{}^4A_{1g}$ multiplets. This problem has been discussed many times in the literature (Refs. 7, 9, 17, 20, 22, 23–25, 27, 43, and 75–77) and has been considered a critical feature of the spectral analysis of the MnF_6^{4-},[9] owing to its relation with the covalency and electronic delocalization in this cluster. We have studied this relation by analyzing several covalency schemes in the light of our SCF results at different values of R.

These two states are degenerate in the simpler form of the crystal-field theory. If the Racah parameters are not fixed at the free-ion values but determined from the observed spectrum this degeneracy remains. In the covalency-factor scheme of Koide and Pryce,[77] where the Racah parameters are assigned their free-ion values and the observed reduction in term energies is accounted for by a covalency factor, the degeneracy can be removed. Also, as discussed by Lohr,[75] two different covalency factors, $f(t_{2g})$ and $f(e_g)$, can be introduced as variable parameters in order to reproduce the observed spectrum. Moreover, Ferguson[9] suggested that very good agreements with the observed transitions could be obtained if different covalency factors are assigned to different ligand field levels. This approach, however, gives rise to an undesirably large number of fitting parameters.

Here we analyze two families of covalency schemes. The first family includes three well-known two-parameter theories: the radial expansion model of Marshall and Stuart,[78] the normalization-constant approach of Curie *et al.*,[76] and a nephelauxetic-effect model. Within this group of schemes we compute the Lohr $f(t_{2g})$ and $f(e_g)$ parameters[75] by means of appropriate transformations of our SCF MO's. We then obtain the splitting energy $\Delta E=E(^4E_g^a)-E(^4A_{1g})$ in terms of $f(t_{2g})$ and $f(e_g)$. In the second family of covalency schemes we examine the MO descriptions already discussed: CI, CI plus CECr, and CI plus CECd, that for brevity will be called now $D1$, $D2$, and $D3$, respectively.

The study of the first group of schemes requires the orbital transformations that we summarize as follows.

(A) The $3d$-expansion scheme neglects any metal-ligand mixing and relates the covalency to the *radial expansion* parameter w: $|3d(r)\rangle \rightarrow |3d(wr)\rangle$.[78] The transformation of our open-shell MO's,

$$|2t_{2g}\rangle = a\,|3d_M\rangle + b\,|3d_I\rangle + c\,|\chi_\pi\rangle$$
$$\rightarrow N_t^w[\,|3d(w)\rangle - \lambda_\pi^w\,|\chi_\pi\rangle\,]$$

gives $w = w(t_{2g})$. In an analogous manner we find $w(e_g)$. The covalency factors are $f(e_g) = w(e_g)^{1/2}$, $f(t_{2g}) = w(t_{2g})^{1/2}$.

(B) In the *normalization-constant* approach[76] the metal-ligand mixing is recognized and the covalency is represented by the coefficient of the $3d$ function in the MO. The transformation,

$$|2t_{2g}\rangle = a\,|3d_M\rangle + b\,|3d_I\rangle + c\,|\chi_\pi\rangle$$
$$\rightarrow N_t(\,|3d_M\rangle - \lambda_\pi\,|\chi_\pi\rangle)$$

now gives N_t and then $f(t_{2g}) = N_t^2$. Analogously, $f(e_g) = N_e^2$.

(C) The *nephelauxetic-effect* model considered here appears when we reduce the ten independent two-electron integrals to the following effective parameters:

$$w(tt) = [3\bar{J}(tt) - 3\bar{K}(tt)]/(2A_0 - 10B_0)\,,$$

$$w(ee) = [2\bar{J}(ee) - 2\bar{K}(ee)]/(A_0 - 8B_0)\,,$$

where A_0, B_0 are free-ion Racah parameters. We now have $f(t_{2g}) = w(tt)^{1/2}$, $f(e_g) = w(ee)^{1/2}$.

In Fig. 3 we present the R dependence of $f(t_{2g})$ and $f(e_g)$ computed with the schemes A, B, and C. In Fig. 4 we plot the corresponding values of ΔE. Noticeable differences appear among these three schemes. However, $f(t_{2g})$ is smaller than $f(e_g)$ for practically all cases and, as Lohr noted,[75] $\Delta E < 0$ when $f(e_g) > f(t_{2g})$. It is interesting to note that if $R \rightarrow 4.0$ a.u., the results of these schemes tend to coincide, the covalency factors f tend to unity, and ΔE remains negative. Therefore, according to these schemes, the ${}^4E_g^a$ lies below the ${}^4A_{1g}$, as a consequence of a σ delocalization larger than the π delocalization.

From Fig. 4 we deduce that the three MO schemes of covalency discussed here give the same picture of the splitting energy of the ${}^4E_g^a, {}^4A_{1g}$ states. Although this quantity turns out to be negative for $R \leq 3.9$ a.u., it becomes positive in the equilibrium region, in contrast with the predictions of the two-parameter approaches and with Ferguson's assignment.[9] From the point of view of the simpler f-factor approach, this change of sign of ΔE would represent a change in the relative values of the π and σ covalency. However, the structure of the open-shell MO's reveals a σ covalency larger than the π covalency. Therefore, the relation found in the more refined calcula-

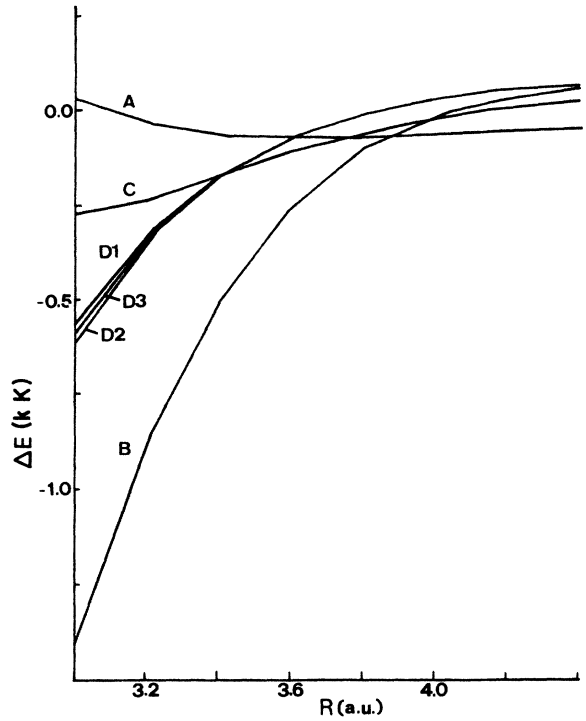

FIG. 3. e_g (solid lines) and t_{2g} (dashed lines) covalency factors versus metal-ligand separation computed with three different covalency schemes. A: Radial expansion scheme. B: normalization-constant scheme. C: nephelauxetic-effect scheme.

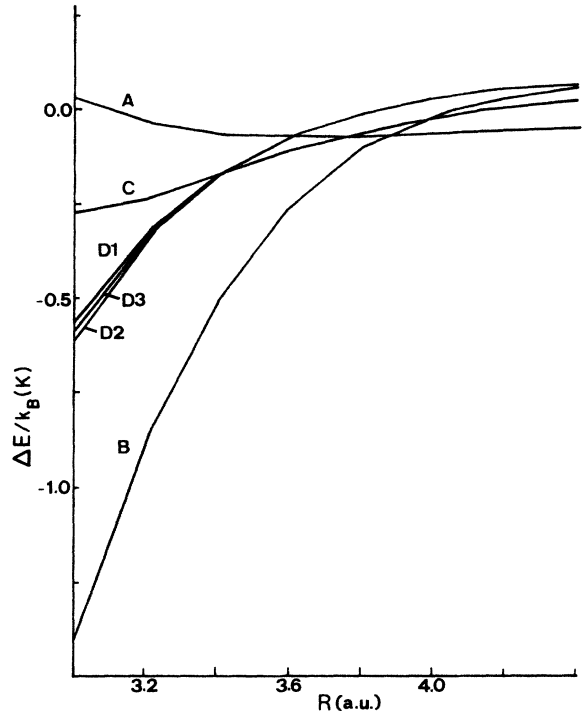

FIG. 4. Splitting energy $\Delta E = E({}^4E_g^a) - E({}^4A_{1g})$ versus metal-ligand separation computed with six different covalent schemes. A, B, and C labels have the same meaning as in Fig. 3. $D1$, $D2$, and $D3$ correspond to the names given in the text.

tion between ΔE and the covalency of the cluster turns out to be different from, and essentially more complex than, that deducible from the crystal-field schemes. In the case investigated here we have a σ covalency larger than the π covalency at any value of R, but a ΔE which changes sign at about $R=3.9$ a.u. This difference between crystal-field and MO schemes could be expected because in the latter we are dealing with ten repulsion integrals and with the CEC as well. Given the different R dependence of the t_{2g}-t_{2g} and e_g-e_g repulsion parameters mentioned above, it is not at all evident that quantities such as ΔE or the theoretical Racah integrals, determined by these parameters, should have a variation with R analogous to that shown by the MO coefficients of a particular MO. Accordingly, the relationship between this type of quantity and the covalency measured through the coefficients of specific MO's is not immediately clear, for a given transition-metal system.

ACKNOWLEDGMENTS

We are grateful to Professor M. Moreno of the University of Santander, Spain, for fruitful discussions and a critical reading of the manuscript. Financial support from the Comisión Asesora de Investigación Científica y Técnica (CAICyT), Spain (Grant No. 2882/83) is gratefully acknowledged.

*Present address: Department of Chemistry, The University of Alberta, Edmonton, Alberta, Canada T6G 2G2.

[1]J. W. Stout, J. Chem. Phys. **31**, 709 (1959).
[2]D. M. Finlayson, I. S. Robertson, T. Smith, and R. W. H. Stevenson, Proc. Phys. Soc. London **76**, 355 (1960).
[3]W. W. Holloway, Jr., M. Kestigian, R. Newman, and E. W. Prohofsky, Phys. Rev. Lett. **11**, 82 (1963).
[4]V. V. Eremenko and A. I. Belyaera, Fiz. Tverd. Tela (Leningrad) **10**, 2877 (1963) [Sov. Phys.—Solid State **5**, 2106 (1964)].
[5]W. Low and G. Rosengarten, J. Mol. Spectrosc. **12**, 319 (1964).
[6]W. W. Holloway, Jr., E. W. Prohofsky, and M. Kestigian, Phys. Rev. **139**, 954 (1965).
[7]R. Stevenson, Can. J. Phys. **43**, 1732 (1965).
[8]D. D. Sell, R. L. Greene, and R. M. White, Phys. Rev. **158**, 489 (1967).
[9]J. Ferguson, Aust. J. Chem. **21**, 307 (1968).
[10]R. S. Meltzer and L. L. Lohr, Jr., J. Chem. Phys. **49**, 541 (1968).
[11]R. L. Greene, D. D. Sell, R. S. Feigelson, G. F. Imbusch, and H. J. Guggenheim, Phys. Rev. **171**, 600 (1968).
[12]A. Mehra, J. Phys. Chem. **75**, 435 (1971).
[13]S. E. Stokowski and D. D. Sell, Phys. Rev. B **3**, 208 (1971).
[14]S. E. Stokowski, D. D. Sell, and H. J. Guggenheim, Phys. Rev. B **4**, 3141 (1971).
[15]J. M. Flaherty and B. Di Bartolo, Phys. Rev. B **8**, 5232 (1973).
[16]B. A. Wilson, W. M. Yen, J. Hegarty, and G. F. Imbusch, Phys. Rev. B **19**, 4238 (1979).
[17]J. Ferguson, H. J. Guggenheim, and Y. Tanabe, J. Appl. Phys. **36**, 1046 (1965).
[18]J. Ferguson, H. J. Guggenheim, and Y. Tanabe, Phys. Rev. Lett. **14**, 737 (1965).
[19]J. Ferguson, H. J. Guggenheim, and Y. Tanabe, J. Phys. Soc. Jpn. **21**, 692 (1966).
[20]R. Stevenson, Phys. Rev. **152**, 531 (1966).
[21]W. E. Vehse and W. A. Sibley, Phys. Rev. B **6**, 2443 (1972).
[22]H. Komura, V. C. Srivastava, and R. Stevenson, Phys. Rev. B **8**, 377 (1973).
[23]H. Komura, M. M. Shapiro, and R. Stevenson, Phys. Rev. B **9**, 3266 (1974).
[24]V. C. Srivastava and R. Stevenson, Solid State Commun. **11**, 41 (1972).
[25]A. Mehra and P. Venkateswarlu, J. Chem. Phys. **47**, 2334 (1967).
[26]M. V. Iverson and W. A. Sibley, Phys. Rev. B **21**, 2522 (1980).
[27]J. P. Srivastava and A. Mehra, J. Chem. Phys. **57**, 1587 (1972).
[28]A. V. Malakhovskii and G. G. Vasil'ev, Fiz. Tverd. Tela (Leningrad) **24**, 585 (1982) [Sov. Phys.—Solid State **24**, 328 (1982)].
[29]P. J. Alonso, V. M. Orera, F. Palacio, and R. Alcalá, Phys. Status Solidi B **109**, k81 (1982).
[30]T. Tsuboi and W. Kleemann, Phys. Rev. B **27**, 3762 (1983).
[31]S. I. Yun, K. H. Lee, W. A. Sibley, and W. E. Vehse, Phys. Rev. B **10**, 1665 (1974).
[32]K. H. Lee and W. A. Sibley, Phys. Rev. B **12**, 3392 (1975).
[33]H. U. Güdel, Chem. Phys. Lett. **36**, 328 (1975).
[34]J. Ferguson, H. J. Guggenheim, and Y. Tanabe, Phys. Rev. **161**, 207 (1967).
[35]D. T. Palumbo and J. J. Brown, Jr., J. Electrochem. Soc. **118**, 1159 (1971).
[36]S. I. Yun, L. A. Kappers, and W. A. Sibley, Phys. Rev. B **8**, 773 (1973).
[37]W. A. Sibley and N. Koumvakalis, Phys. Rev. B **14**, 35 (1976).
[38]D. K. Sardar, M. D. Shinn, and W. A. Sibley, Phys. Rev. B **26**, 2382 (1982).
[39]M. Moreno, F. Rodríguez, J. A. Aramburu, F. Jaque, and F. J. López, Phys. Rev. B **28**, 6100 (1983).
[40]A. J. Freeman and D. E. Ellis, Phys. Rev. Lett. **24**, 516 (1970).
[41]T. F. Soules and J. W. Richardson, Phys. Rev. Lett. **25**, 110 (1970).
[42]O. Matsuoka, J. Phys. Soc. Jpn. **28**, 1296 (1970); **30**, 1771 (1971).
[43]L. L. Lohr, Jr., J. Chem. Phys. **55**, 27 (1971).
[44]S. Larsson and J. W. D. Connolly, Chem. Phys. Lett. **20**, 323 (1973).
[45]S. Larsson and J. W. D. Connolly, J. Chem. Phys. **60**, 1514 (1974).
[46]H. Adachi, S. Shiokawa, M. Tsukada, C. Satoko, and S. Sugano, J. Phys. Soc. Jpn. **47**, 1528 (1979).
[47]J. Emery, A. Leble, and J. C. Fayet, J. Phys. Chem. Solids **42**, 789 (1981).
[48]J. Emery and J. C. Fayet, Solid State Commun. **42**, 683 (1982).
[49]J. W. Richardson, T. F. Soules, D. M. Vaught, and R. R. Powell, Phys. Rev. B **4**, 1721 (1971).
[50]J. W. Richardson, D. M. Vaught, T. F. Soules, and R. R. Powell, J. Chem. Phys. **50**, 3633 (1969).
[51]T. F. Soules, J. W. Richardson, and D. M. Vaught, Phys. Rev. B **3**, 2186 (1971).
[52]B. L. Kalman and J. W. Richardson, J. Chem. Phys. **55**, 4443 (1971).
[53]L. Pueyo and J. W. Richardson, J. Chem. Phys. **67**, 3583

(1977).
[54]L. Seijo, L. Pueyo, and F. Gómez Beltrán, J. Solid State Chem. **42**, 28 (1982).
[55]S. Gutiérrez Orellana and L. Pueyo, J. Solid State Chem. **55**, 30 (1984).
[56]Z. Barandiarán, L. Pueyo, and F. Gómez Beltrán, J. Chem. Phys. **78**, 4612 (1983).
[57]Z. Barandiarán and L. Pueyo, J. Chem. Phys. **79**, 1926 (1983).
[58]Z. Barandiarán and L. Pueyo, J. Chem. Phys. **80**, 1597 (1984).
[59]L. Pueyo, M. Bermejo, and J. W. Richardson, J. Solid State Chem. **31**, 217 (1980).
[60]L. Seijo and L. Pueyo, J. Solid State Chem. **56**, 241 (1985).
[61]J. W. Richardson, W. C. Nieuwpoort, R. R. Powell, and W. F. Edgell, J. Chem. Phys. **36**, 1057 (1962).
[62]J. W. Richardson, R. R. Powell, and W. C. Nieuwpoort, J. Chem. Phys. **38**, 796 (1963).
[63]L. Seijo, Doctorate thesis dissertation, University of Oviedo, 1983.
[64]J. S. Griffith, *The Theory of Transition-Metal Ions* (Cambridge University Press, London, 1971).
[65]R. R. Sharma, M. H. de A. Viccaro, and S. Sundaram, Phys. Rev. B **23**, 738 (1981).
[66]R. R. Sharma and S. Sundaram, Solid State Commun. **33**, 381 (1980).
[67]L. Pueyo and J. W. Richardson, J. Chem. Phys. **67**, 3577 (1977).
[68]C. E. Moore, U.S. National Bureau of Standards Circular No. 467, Vol. 2, 1952.
[69]O. García-Riquelme, Opt. Pura Apl. **1**, 53 (1968).
[70]M. B. Walker and R. W. H. Stevenson, Proc. Phys. Soc. London **87**, 35 (1966).
[71]R. E. Trees and C. K. Jørgensen, Phys. Rev. **123**, 1278 (1961), and the references quoted therein.
[72]Consideration of a smaller range of R, in the neighborhood of the equilibrium nuclear configuration, would increase this value of n. We are indebted to Professor M. Moreno for this observation.
[73]M. T. Barriuso and M. Moreno, Phys. Rev. B **29**, 3623 (1984).
[74]E. Dormann, D. Hone, and V. Jaccarino, Phys. Rev. B **14**, 2715 (1976).
[75]L. L. Lohr, Jr., J. Chem. Phys. **45**, 3611 (1966).
[76]D. Curie, C. Barthou, and B. Canny, J. Chem. Phys. **61**, 3048 (1974).
[77]S. Koide and M. L. H. Pryce, Philos. Mag. **3**, 607 (1958).
[78]W. Marshall and R. Stuart, Phys. Rev. **123**, 2048 (1961).